

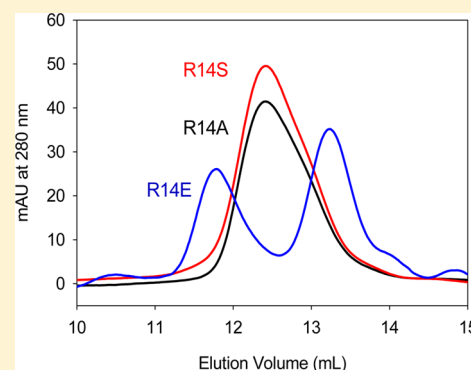
Basic Residue at Position 14 Is Not Required for Fast Assembly and Disassembly Kinetics in Neural Cadherin

Nagamani Vunnam,* Nathan I. Hammer, and Susan Pedigo

Department of Chemistry and Biochemistry, University of Mississippi, University, Mississippi 38677, United States

Supporting Information

ABSTRACT: In spite of their structural similarities, epithelial (E-) and neural (N-) cadherin are expressed at different types of synapses and differ significantly in their dimerization kinetics. Recent studies proposed a transient intermediate in E-cadherin as the key requirement for rapid disassembly kinetics of the adhesive dimer. This E-cadherin intermediate comprises four intermolecular ionic and H-bonding interactions between adhesive partners. These interactions are not preserved in N-cadherin except for a basic residue at the 14th position, which could stabilize the intermediate through either H-bonding or ionic interactions with the partner protomer. To investigate the origin of the rapid dimerization kinetics of N-cadherin in the presence of calcium, studies reported here systematically test the role of ionic and H-bonding interactions in dimerization kinetics using R14S, R14A, and R14E mutants of N-cadherin. Analytical size-exclusion chromatographic and bead aggregation studies showed two primary results. First, N-cadherin/R14S and N-cadherin/R14A mutants showed fast assembly and disassembly kinetics in the calcium-saturated state similar to that of wild-type N-cadherin. These results indicate that the fast disassembly of the calcium-saturated dimer of N-cadherin does not require a basic residue at the 14th position. Second, the dimerization kinetics of N-cadherin/R14E were slow in the calcium-saturated state, indicating that negative charge destabilizes the intermediate state. Taken together, these results indicate that the basic residue at the 14th position does not promote rapid dimerization kinetics but that an acidic amino acid in that position significantly impairs dimerization kinetics.



Cadherins are the primary cell–cell adhesion molecules in solid tissues. Adhesion by cadherins is calcium-dependent and occurs via association between like molecules on adjacent cells in adherens junctions. In the developed brain, different members of the cadherin family are expressed at specific locations.^{1–3} Neural (N-) cadherin is specifically expressed at excitatory synapses and is important in long-term potentiation,^{4–6} whereas epithelial (E-) cadherin occurs at inhibitory synapses. In carcinomas, decreased expression of E-cadherin with a concomitant expression of N-cadherin is a hallmark for metastasis.⁷ This segregation of cadherins into distinct physiological milieu implies distinct function. Although these two prominent members of the classical cadherin family differ by a factor of 4 in their equilibrium dimerization affinity,⁸ the most striking difference is in the calcium dependence of dimerization kinetics. Adhesive dimers of E-cadherin are in rapid exchange with monomers, regardless of the concentration of calcium, whereas the kinetics of dimerization by N-cadherin are rapid only in the presence of calcium.⁹ Here, we test the applicability of a current model for rapid dimerization kinetics in E-cadherin to the kinetics of adhesive dimer formation mediated by N-cadherin.

Classical cadherins comprise an extracellular (EC) region with five tandem extracellular domains (EC1–5) that bind calcium, a transmembrane segment, and a conserved C-terminal cytoplasmic region.^{10–12} Cell–cell adhesion occurs through the formation of adhesive dimers comprising an N-terminal strand

exchange between the EC1 domains of cadherins from neighboring cells.^{13,14} Recent crystallographic and cell adhesion studies of E-cadherin proposed an intermediate, low-affinity dimeric structure between component protomers, the X-dimer, which is necessary for fast disassembly of the adhesive dimer.^{15,16} Of the four noncovalent interactions originally proposed to comprise the X-interface, attention has been focused on the ionic interaction between K14 and D138 on partner protomers as being necessary for rapid exchange between monomer and dimer.^{15,16} Studies have shown that the charge-change mutation K14E had no effect on the equilibrium dimerization affinity, even though the kinetics of assembly and disassembly in wild-type E-cadherin were 10 000-fold faster than those in the charge-change mutant,¹⁷ illustrating that the presence of glutamate in position 14 has a profound effect on dimerization in E-cadherin.

As mentioned above, N- and E-cadherin differ significantly in disassembly kinetics *in vitro*^{9,18–20} and *in vivo*.²¹ Whereas the disassembly of E-cadherin dimers is rapid in the presence or absence of calcium,^{9,18–20} the disassembly of N-cadherin dimers is strongly calcium-dependent. N-cadherin has two distinct dimeric forms: a fast-exchange calcium-saturated dimer

Received: August 19, 2014

Revised: December 12, 2014

Published: December 17, 2014

(D_{satd}) and a kinetically trapped apo-dimer (D_{apo}^*).⁹ Interestingly, all four of the X-interface interactions proposed for E-cadherin are absent in N-cadherin due to sequence differences between the two proteins (Figure 1). In a previous publication,

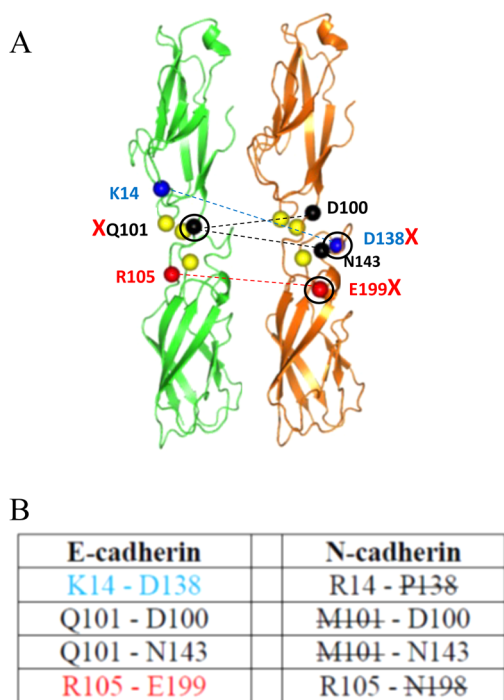


Figure 1. Comparison of X-interface amino acids in E- and N-cadherin. (A) Schematic depicting the interactions at the X-interface in E-cadherin. Ribbon drawing of the first two domains of E-cadherin (PDB ID: 1FF5⁴⁶) illustrating the four X-dimer interactions.¹⁵ Calcium ions are shown as spheres (yellow). Residues circled in black with a red X by their label are not conserved in N-cadherin. (B) Amino acids that participate in X-dimer interactions in E-cadherin and those in the analogous position in N-cadherin. Adapted from ref 22. Copyright 2012 The Protein Society.

we addressed the question of whether the absence of these specific interactions is responsible for the slow disassembly kinetics of D_{apo}^* in N-cadherin.²² We introduced three point mutations into N-cadherin to provide the opportunity for the formation of all four X-interface interactions proposed for E-cadherin and found no effect on the kinetics of N-cadherin in the absence of calcium. In the current work, we study the origin of fast dimerization kinetics of calcium-saturated N-cadherin dimer. Here, we address whether R14, the basic residue in position 14 in N-cadherin, has a similar role in facilitating rapid kinetics of dimerization in the presence of calcium, as was witnessed for K14 in E-cadherin.

The general concept of an X-dimer¹⁵ or initial encounter complex²³ is useful for explaining observed phenomena related to strand-crossover dimer formation. The face-to-face association of protomers in an intermediate structure prior to strand exchange explains why we observe only cadherin dimers and not daisy-chain oligomers. In addition, formation of the strand-swapped dimer requires that the critical tryptophan in the second position,²⁴ W2, undocks from the closed monomer in order for the β A-strands to exchange. Exposure of W2 to a more polar environment was not observed in steady-state tryptophan fluorescence emission studies.²⁵ This result is consistent with the idea that the strand-swapped interface

remains buried in the intermediate during strand exchange, as would be expected in a face-to-face close-encounter complex. Moreover, as proposed elsewhere, the X-dimer would function to stabilize the transition state between the closed monomer and the closed, strand-swapped dimer.^{17,23,26} Crystallographic studies provided the molecular details for the intermediate structure (X-dimer) in E-cadherin (Figure 1). No similar structure for N-cadherin has been solved. However, the conservation of a basic residue in position 14 in N-cadherin, and its apparent necessity for fast dimer exchange in E-cadherin, implicate this residue as a critical player for the fast exchange observed for N-cadherin dimers in the presence of calcium.

Since all of the X-interface interactions for E-cadherin are absent in N-cadherin, those particular interactions cannot explain the observed fast disassembly of D_{satd} of N-cadherin.⁹ The role of one key residue in N-cadherin, R14, needs to be explored. Although N-cadherin lacks D138 (P138 in N-cadherin) as an interaction partner for R14, other possibilities need to be considered. Arginine 14 in N-cadherin may have ionic interactions with D137, as proposed by Harrison et al.,¹⁵ or H-bond with the backbone carbonyls in the region of residue 138. There are two precedents in the literature for H-bonding of residues in position 14 with the backbone carbonyl at position 138. These include modeling based on crystallographic evidence for H-bonding of the side chain hydroxyl of T14 with the carbonyl of P138 in Cadherin-6,¹⁵ a type II cadherin, and the H-bonding or ionic interaction of R14 with the side chain of D140 in T-cadherin, a nonclassical cadherin.²⁷ In order to address the requirement for R14 in N-cadherin in the rapid kinetics of dimerization, we created three mutants of R14, namely, R14S, R14A and R14E. Here, we report the effect of these mutations on the kinetics of dimerization in N-cadherin.

EXPERIMENTAL PROCEDURES

Cloning and Protein Expression. We created six different constructs comprising EC1 and EC2 of N-cadherin (residues 1–221): NCAD12/WT, NCAD12/R14S, NCAD12/R14A, NCAD12/R14E, NCAD12/X-enabled, which is a triple mutant of N-cadherin (M101Q/P138D/N198E) that introduces all of the components necessary to form the four pairwise interactions in the X-interface, and, finally, NCAD12/X-enabled/R14E.^{9,22} The mutant constructs were created by site-directed mutagenesis of the NCAD12/WT plasmid using the Quik Change kit (Stratagene). Amplification of the two-domain constructs, digestion of template DNA, ligation into pET30 Xa/LIC, and subsequent transformation into *Escherichia coli* BL21 (DE3) were performed according to standard protocols, utilizing KOD HiFi DNA polymerase (Stratagene) and the Xa/LIC cloning kit (Novagen). The mutations were confirmed by sequencing of plasmid DNA. For bead aggregation studies, the stop codon following EC2 was mutated to a glutamine to create a C-terminal fusion of 26 amino acids including a His₆ sequence. An additional mutation was made to remove a lysine from the C-terminal fusion in order to prevent cleavage of the C-terminal His₆ sequence by trypsin.

Protocols for protein overexpression and purification were described previously.⁹ Purity of proteins was assessed by SDS-PAGE in 17% polyacrylamide gels. Extinction coefficients were determined experimentally²⁸ at 280 nm to be $15\,500 \pm 600 \text{ M}^{-1} \text{ cm}^{-1}$ for the NCAD12 constructs used in the current studies.

Thermal-Unfolding Studies. Thermal unfolding of all six constructs was monitored with an AVIV 202SF CD spectrometer. Experimental conditions were described in our previously published work.⁹ To monitor the effect of calcium binding on protein stability, studies were performed at two calcium concentrations (apo, 50 μ M EDTA; calcium-saturated state, 1 mM) in 140 mM NaCl, 10 mM HEPES, pH 7.4. The thermal-denaturation transitions were fit to the Gibbs–Helmholtz equation as described previously.²⁹

Bead Aggregation Studies. *Aggregation of Cadherin-Coated Beads.* Dimerization of all four cadherin constructs was tested by observing the aggregation of cadherin-coated beads in the presence of calcium as a function of incubation time. A 5 μ L volume of Dynabead solution was transferred into a 1.5 mL microfuge tube and rinsed four times in 70 μ L of binding buffer (100 mM Na-Phosphate, pH 8.0, 600 mM NaCl, 0.02% Tween). Next, 250 μ L of 1.7 μ M NCAD12 stock in binding buffer was added to the beads, and beads were incubated at 4 °C for 30 min. Protein-coated beads were settled on a magnet, and the overlaying solution was removed and rinsed twice with 250 μ L of assay buffer (10 mM HEPES, 140 mM NaCl, 1 mM CaCl₂, pH 7.4) with 0.2% BSA. Samples were incubated without agitation. Before placing 10 μ L of sample on the slide for microscopic analysis, we mixed the sample 10 times by aspiration with a 100 μ L pipet. The bead images were taken with a 10 \times objective and a CCD camera (ProEm 1024) on a Nikon Eclipse TE 2000-U microscope. WinView Imaging software (Princeton Instrument, ver. 2.5) was used to acquire the data from the CCD camera. In order to quantitatively analyze the bead aggregation data, WinView Imaging files were saved in an 8-bit TIFF format to transfer the data into ImageJ (rsbweb.nih.gov/ij/), which was used for advanced processing of the images.

Sedimentation Rate of Cadherin Coated Beads. We developed a new bead aggregation method to study the association rate of cadherin. In this method, we monitor sedimentation of cadherin-coated beads due to gravity. Optical density (OD) was recorded at 5 min intervals for 60 min at 600 nm in the presence of calcium (1 mM). The half-time ($t_{1/2}$) for sedimentation was determined by plotting the OD reading at 600 nm as a function of time. Since the dimerization affinity is similar for the mutants, the half-time is reciprocally related to the sedimentation rate and association rate of the cadherin-coated beads; a short half-time indicates that the dimerization is fast.

Analytical Size-Exclusion Chromatography (SEC) Studies. Analytical SEC was used to evaluate the overall differences in the kinetics of dimer disassembly of all four constructs in the apo (140 mM NaCl, 10 mM HEPES, pH 7.4) and calcium (140 mM NaCl, 10 mM HEPES, 1 mM calcium, pH 7.4) mobile phases. These experiments were performed using an ÄKTA Purifier HPLC (GE Life Sciences) with a Superose-12 10/300 GL Column (GE Life Sciences) with detection at 280 nm and a 0.5 mL/min flow rate. The column volume is \sim 25 mL, and the total time to elute monomer was \sim 30 min. Calibration of the SEC column was described previously.⁹ Each experiment was repeated at least three times.

Qualitative Assessment of the Effect of Calcium on the Disassembly of Dimer. To qualitatively illustrate the exchange rate between monomer and dimer as a function of calcium concentration, protein samples in 1 mM calcium were injected on the SEC column in both the apo- and calcium-mobile phases (\sim 1 μ M and 1 mM). A single peak in the chromatogram

indicates that the exchange between monomer and dimer is rapid, and two peaks indicate that the exchange is slow.

Characterization of Assembly of Dimer as a Function of Incubation Time. To observe the formation of dimer as a function of time, 40 μ M protein samples in 1 mM calcium were injected on the SEC column in apo-mobile phase at different time intervals, ranging from 30 min to days. N-cadherin forms a kinetically trapped dimer (D_{apo}^*) upon rapid decalcification of the calcium-saturated dimer (D_{satd}). Chromatographic analysis of the level of the D_{apo}^* can be used to determine the K_d for dimerization in the presence of calcium.⁹ Thus, to observe the level of calcium-saturated dimer present in the 40 μ M sample, 5 mM EDTA was added to each sample to form the trapped dimer, which was incubated for 30 min prior to injection on the SEC column. We monitored the assembly kinetics by observing the increase in the level of dimer as a function of time before addition of EDTA. The second-order kinetic data for the R14E mutants were analyzed by eqs 1 and 2 to yield an observed association rate constant, k_{obs} , and the equilibrium dissociation constant, K_d .

$$[M] = 1 / \left(\frac{1}{[M]_0} + k_{obs}t \right); \quad 2[D] = [M]_0 - [M] \quad (1)$$

$$K_d = \frac{[M]^2}{[D]} \quad (2)$$

$[M]_0$ is the initial protein concentration. K_d was determined for all constructs from $[D]$ and $[M]$ according to eq 2. The time constant for dimerization, τ , is a function of the concentration of protein in solution, as shown in eq 3.

$$\tau = \frac{[\text{protein}]}{k_{obs}} \quad (3)$$

RESULTS

To address whether the X-dimer paradigm as defined in E-cadherin applies to the kinetics of dimerization of N-cadherin, we created three different constructs with mutations of R14 only: NCAD12/R14A, NCAD12/R14S, and NCAD12/R14E. We also examined a triple mutant of N-cadherin (M101Q/P138D/N198E), which has all of the component interactions that form the X-interface in E-cadherin (NCAD12/X-enabled). This mutant is a control for direct comparison of wild-type N-cadherin to E-cadherin. A second mutant, NCAD12/X-enabled/R14E with four mutations (R14E/M101Q/P138D/N198E), is a control for direct comparison to E-cadherin K14E; all X-dimer components are present except for the basic residue in position 14. Comparison of assembly and disassembly kinetics of these six constructs will address whether the X-dimer model, as defined from crystallographic studies of E-cadherin,¹⁵ applies to the kinetics of dimerization of N-cadherin.

Thermal-Unfolding Studies. Thermal-unfolding studies were performed to assess whether the mutations had an effect on the structure and stability of the protein. Thermal-unfolding data of all six proteins showed two transitions: the first results from the denaturation of EC2,³⁰ and the second, from the denaturation of EC1³¹ (Supporting Information Figure S1). Only the first transition was stabilized by addition of calcium. Data for the first transition was fitted to the Gibbs–Helmholtz equation. Interestingly, whereas the stability of NCAD12/X-enabled, NCAD12/R14A, NCAD12/R14S, and NCAD12/

R14E was similar to that of NCAD12/WT, the combination of the X-enabling and R14E mutations significantly decreased the stability of EC2 (Supporting Information Table S1). The NCAD12/X-enabled/R14E construct has three additional negative charges in comparison to NCAD12/WT. Thus, this construct may be destabilized due to increased electrostatic repulsion.

Analytical Size-Exclusion Chromatography (SEC) Studies. Qualitative Assessment of the Effect of Calcium on the Disassembly of Dimer. Analytical SEC was used to monitor the impact of the X-interface mutations on the disassembly kinetics of monomer–dimer equilibria in the presence of calcium. Analysis of calcium-added samples in a calcium-added mobile phase yielded a single peak for NCAD12/R14A and NCAD12/R14S with an intermediate elution volume, as seen for NCAD12/WT (Figure 2),

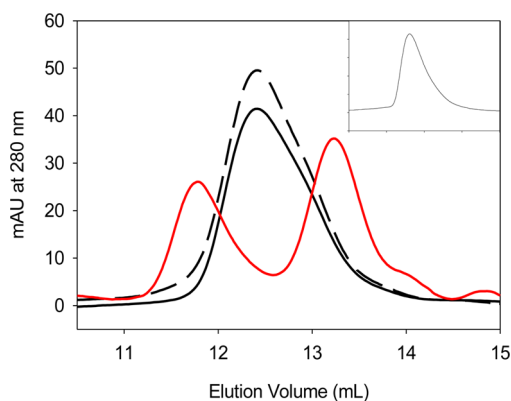


Figure 2. Assessment of monomer–dimer exchange kinetics in the presence of calcium using analytical SEC. Calcium-saturated NCAD12/R14S (red), NCAD12/R14A (black), and NCAD12/R14E (blue) protein samples ($\sim 20 \mu\text{M}$) were injected on the SEC column and analyzed under calcium-added mobile phase conditions. Inset: calcium-saturated NCAD12/WT.

indicating that the monomer–dimer equilibrium is rapid in the presence of calcium and independent of the X-interface pairwise interactions that were proposed for E-cadherin.¹⁵ Our data show that converting the positively charged (R14) amino acid to a hydrophobic (R14A) or polar (R14S) amino acid does not significantly change the disassembly kinetics, consistent with the idea that ionic and H-bonding interactions by the residue in position 14 are not required for fast disassembly of D_{satd} . In contrast, the construct with the R14E mutation yielded two peaks in the presence of calcium, indicating that the monomer–dimer equilibrium is slow when a glutamate is introduced at the 14th position. Taken together, these results suggest that R14 is not required for fast kinetics in the presence of calcium and that the slow disassembly kinetics observed in the R14E mutant is due to the presence of glutamate rather than the absence of arginine.

Characterization of Assembly of Dimer. The analytical SEC method was used to quantitatively monitor the effect of the X-interface residues on the assembly of dimers. The level of dimer in solution was determined by adding EDTA (5 mM) to protein samples in 1 mM calcium. This procedure effectively creates a snapshot of the level of calcium-saturated dimer in solution at the time that the EDTA was added.⁹ By varying the time intervals before addition of EDTA from 1 min to days, we were able to determine the association rate constant for dimer

assembly. The three protein constructs, NCAD12/WT, NCAD12/R14A, and NCAD12/R14S, showed similar dimer assembly kinetics (Figure 3A–C). The concentration of dimer is plotted in Figure 3 as a function of incubation time. NCAD12/WT, NCAD12/R14A, and NCAD12/R14S reached equilibrium in 0.1 min in the presence of calcium. Moreover, they have similar apparent K_d values for dimerization (Table 1).

The NCAD12/R14E mutant showed significantly delayed dimer assembly kinetics (Figure 3D). Estimates of the pseudo-second-order rate constant (eq 1) for dimer formation were 300 times slower than that found for wild type or for the R14S or R14A mutant. Although the formation of dimer was slow, NCAD12/R14E eventually showed similar dimer levels as that found for NCAD12/WT. Fits of the data to eq 2 yielded values for K_d of the R14E mutant that were similar to the other constructs (Table 1). These results indicate that although the R14E mutation significantly slowed assembly of NCAD12 dimers it did not affect the equilibrium constant for dimerization; a similar result was noted for the K14E and K14S mutants of ECAD12.¹⁵ In summary, these results show that the loss of R14 is inconsequential in the kinetics of dimer disassembly and assembly, with no apparent effect on the equilibrium dissociation constant. However, the gain of negative charge in the charge-change mutant has a profound impact on disassembly kinetics in N-cadherin.

Bead Aggregation Studies. Aggregation of Cadherin-Coated Beads. Dimer assembly of four cadherin constructs was tested by observing the aggregation of cadherin-coated beads in the presence of calcium as a function of incubation time. The advantage of these experiments is that the protomers are tethered by their C-termini to the bead, orienting the protomers as they would be oriented on a cell surface. These studies showed that NCAD12/WT and NCAD12/X-enabled had increased aggregate size after 30 min of incubation (Figure 4). These results indicate that the additional possible interactions at the X-interface in the NCAD12/X-enabled construct have no effect on the dimerization properties. In contrast, the R14E mutants showed no increase in aggregates after 30 min of incubation, indicating that the R14E mutation impacted the dimerization kinetics. After 2 h of incubation for the two R14E mutants, an increase in the cluster size was observed, which indicates that bead association occurs, but the rate is slow. The NCAD12/X-enabled/R14E mutant mimics the X-interactions in the K14E mutant of E-cadherin and is included as a control. In conclusion, the fast assembly kinetics of the calcium-saturated dimer of N-cadherin does not require the pairwise interactions proposed for the X-interface in E-cadherin. Importantly, the slow assembly observed in the R14E mutant indicates that an acidic residue in position 14 has a profound impact on dimerization kinetics.

Sedimentation Rate of Cadherin-Coated Beads. We observed the sedimentation rate of cadherin-coated beads in the presence of calcium (1 mM) as a function of time (Figure 5); the half-time ($t_{1/2}$) for aggregation for all four proteins is reported in Table 2. NCAD12/WT and NCAD12/X-enabled proteins had similar half-times for aggregation, which indicates that these two proteins have similar dimerization kinetics. In contrast, NCAD12/R14E and NCAD12/X-enabled/R14E had higher $t_{1/2}$ than that of NCAD12/WT, again indicating that the presence of glutamate in position 14 impacted the dimerization kinetics.

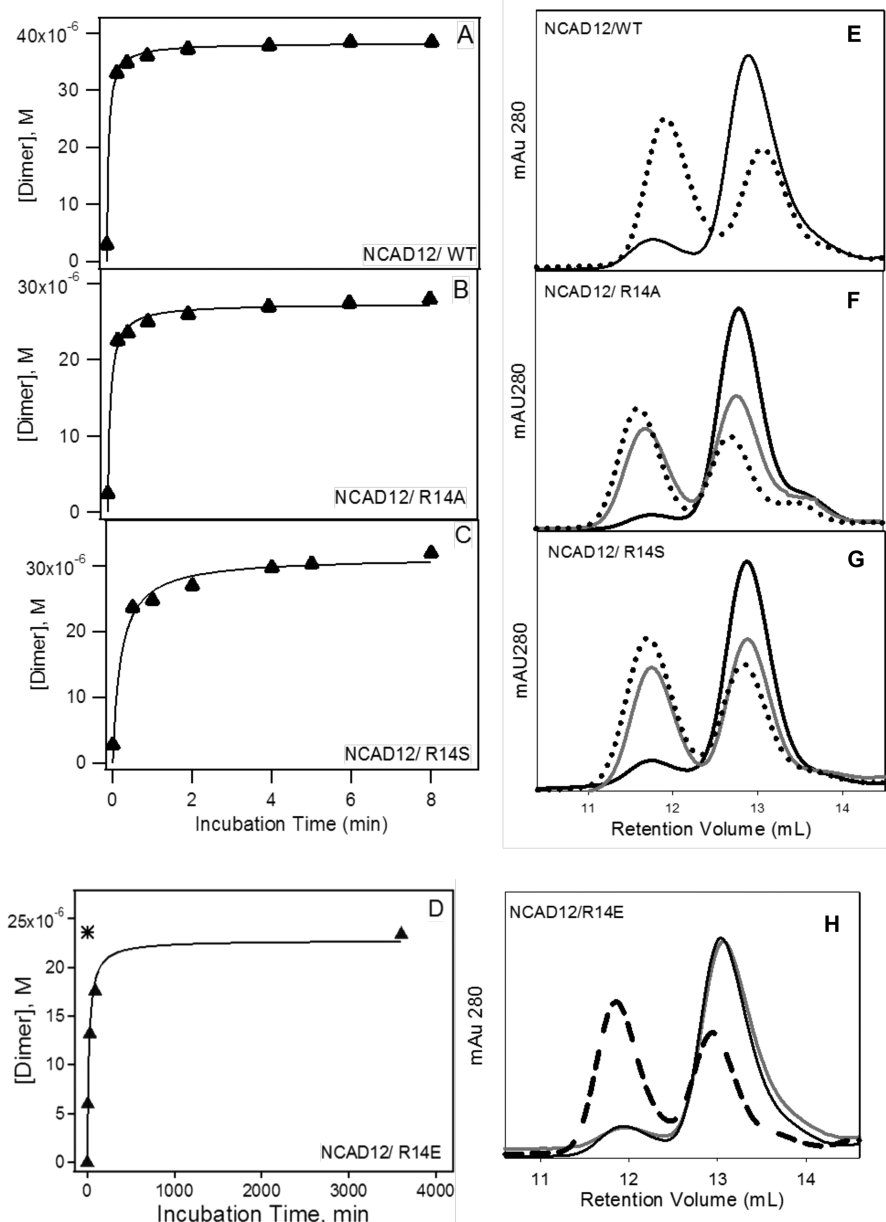


Figure 3. Analytical SEC was used to monitor a time course of dimer formation for all four protein constructs. Concentration of dimer plotted as a function of incubation time for (A) NCAD12/wild type, (B) NCAD12/R14A, (C) NCAD12/R14S, and (D) NCAD12/R14E. Data were fitted to equations eqs 1 and 2 (solid lines). Representative chromatograms for (E) NCAD12/WT, (F) NCAD12/R14A, (G) NCAD12/R14S, and (H) NCAD12/R14E are shown in apo (solid, black) and calcium-added protein samples at different incubation times: 0.5 min, solid, gray; 4 min, dotted, black; and 2 days, dashed, black.

Table 1. Results from Analysis of Kinetic Profiles^a

protein	K_d (μM)	k ($\text{min}^{-1} \text{M}^{-1}$)	Tau (min) ^b
WT	25 ± 2	$(4 \pm 1) \times 10^5$	0.10 ± 0.03
R14A	31 ± 3	$(3 \pm 1) \times 10^5$	0.13 ± 0.04
R14S	33 ± 5	$(1.0 \pm 0.3) \times 10^5$	0.04 ± 0.01
R14E	26 ± 4	$(1.2 \pm 0.3) \times 10^3$	33 ± 8

^aAnalysis of fraction of dimer as a function of time using eqs 1 and 2.

^bTau values at $25 \mu\text{M}$.

DISCUSSION

In the cadherin field, there has been a flurry of interest about the kinetics of formation of the strand-swapped dimer. Particular interest has been focused on the X-dimer structure,

a close-encounter structure that was first observed in crystallographic studies in 1996³² but was later proposed to be functionally significant.¹⁵ The X-dimer structure is a dimer of identical protomers wherein the component molecules are held together by four primary noncovalent interactions that orient the protomers such that the β A-strands can swap,¹⁵ essentially functioning to stabilize the transition state between the closed monomer and the strand-swapped dimer.¹⁷ A rapidly growing body of literature is emerging that focuses on only one of the four interactions, the ionic interaction between K14 and D138 in E-cadherin,^{15,16} N-cadherin,^{22,33} and P-cadherin.³⁴ The studies reported here investigate the requirement for R14 in fast dimerization kinetics of N-cadherin in the presence of calcium.

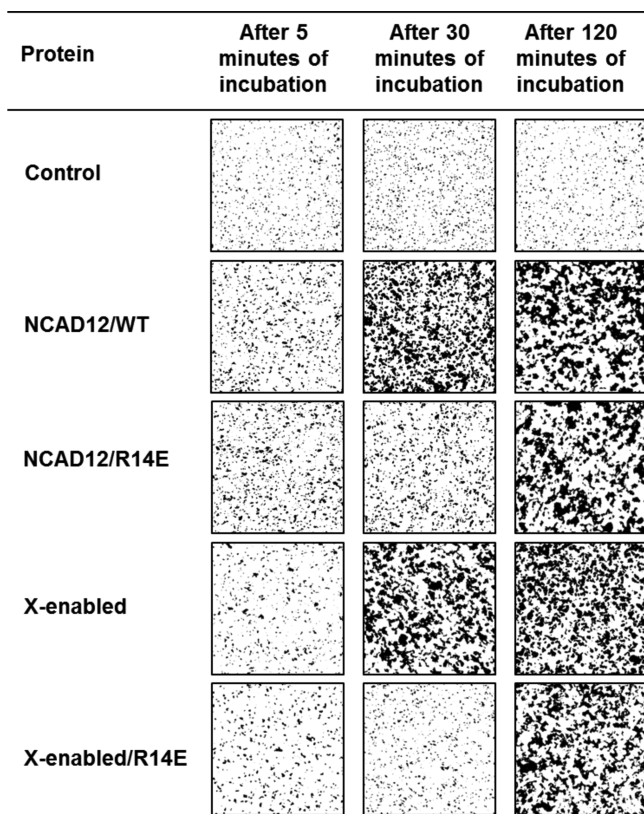


Figure 4. Aggregation of cadherin-coated beads and beads with no protein (control) in the presence of calcium as a function of time. For all four protein constructs, 10 μ L of 1.7 μ M protein-coated bead sample in 1 mM calcium was pipetted on a glass coverslip, and images were taken and processed as described in the text.

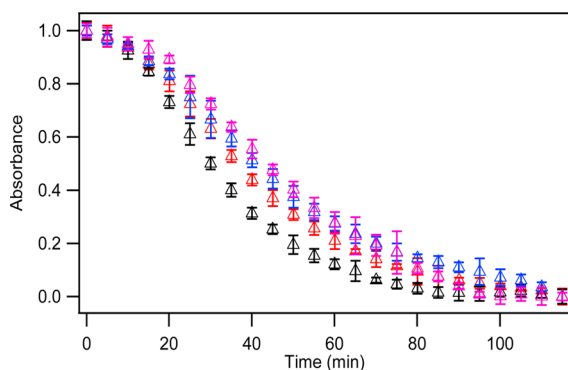


Figure 5. Sedimentation rate of cadherin-coated beads in the presence of calcium (1 mM) as a function of time. Sedimentation rate of cadherin-coated beads, NCAD12/wild type (black), NCAD12/R14E (pink), NCAD12/X-enabled (red), and NCAD12/X-enabled/R14E (blue), was observed by light scattering in a UV spectrophotometer. Optical density (OD) was recorded every 5 min for 60 min at 600 nm.

Table 2. Sedimentation Time for Aggregating Cadherin-Coated Beads

protein constructs	time to reach the midpoint ($t_{1/2}$; min)
NCAD12/WT	29 \pm 2
NCAD12/R14E	42 \pm 4
NCAD12/X-enabled	32 \pm 1
NCAD12/X-enabled/R14E	45 \pm 4

Do the kinetics of dimerization relate to cadherin function? We propose that there is a correlation, but not causal relationship. Dimerization kinetics are calcium-dependent in N-cadherin. First, does calcium concentration fluctuate *in vivo*? Brown et al. argued that there are processes that are regulated according to the fluctuations of calcium ions in the extracellular space.³⁵ Calcium transients in actively firing excitatory synapses have been measured to be as low as 40 μ M,³⁶ supporting the concept that different kinetic regimes will be sampled *in vivo*. In addition, there are microenvironmental factors that could affect calcium-dependent affinity and kinetics of dimerization, including acidification of tissues^{37–43} and competition with other divalent metals.⁴⁴ We argue that the calcium-dependent differences in kinetics of dimerization of E- and N-cadherin are a relevant discussion not only in terms of their *in vivo* function but also as a mechanistic question regarding the formation of an ordered strand-swapped dimeric structure.

The major contribution of this work is the use of biophysical approaches to study the effect of alanine, serine, and glutamate mutants of R14 on the kinetics of dimerization in N-cadherin in the presence of calcium. The analytical SEC method allows us to investigate the assembly and disassembly of the dimer as separate phenomena. The data presented here show that R14 plays no role in the fast assembly and disassembly kinetics in N-cadherin; fast disassembly of the calcium-saturated dimer of N-cadherin does not require any of the proposed interactions from the crystal structure of E-cadherin, including the purported requirement for the basic residue in position 14. In addition, the residue at position 14 can be hydrophobic or an H-bond donor/acceptor without kinetic consequences.

Analytical SEC data showed that the R14S and R14A mutants had similar dimerization kinetics as that of wild type, which indicates that the loss of the arginine in position 14 has no effect on assembly kinetics. In contrast, the glutamate in the 14th position had deleterious effects on both the assembly and disassembly of the dimer in the presence of calcium; the tau value for formation of dimer for the R14E mutant increased from \sim 0.1 min (NCAD12/WT) to 30 min, illustrating the profound impact of the glutamate at this position on assembly kinetics. The time-dependent aggregation of cadherin-coated beads supports this conclusion. In similar bead aggregation studies, Emond et al. also showed the deleterious effect of the R14E mutation in the five domain construct of N-cadherin, reporting no significant dimerization after an hour.³³ Regarding disassembly, we observed slow disassembly of R14E mutants of N-cadherin in the presence of calcium, as witnessed by the distinct difference in the elution volume for monomer and dimer in the SEC experiment, even in the presence of calcium in the mobile phase buffer. These results are very similar to studies of the K14E mutant of E-cadherin reported in work by Harrison et al.¹⁵

Our data indicate that although R14 is not required for the X-dimer the presence of glutamate in that position is debilitating. In crystal structures of N- and E-cadherin, the region in which R14/K14 is located is not constrained by the H-bonding network of a β -sheet. One can imagine that the conformation of that region might be sensitive to the nature of the mutation at position 14. Thus, the penalty paid for a glutamate in position 14 could be due to unfavorable conformation of the surrounding segment, the β A- or β B-strands, that prohibits formation of the intermediate structure. It is also possible that there is repulsion at the X-dimer interface between protomers when glutamate is in position 14. While we

cannot provide a detailed molecular explanation for the effect of the R14E mutation in dimerization kinetics, it is clear that electrostatic repulsion involving anionic residues significantly slows dimerization kinetics, and this repulsive effect precludes formation of the close-encounter intermediate. Studies are underway to determine whether this effect is local or global.

Our current studies show that N-cadherin does not follow the apparent paradigm argued for the X-interface in E-cadherin. Indeed, it is not entirely clear whether E-cadherin really requires K14 for rapid assembly and disassembly given that the K14S mutant of E-cadherin also formed dimer, albeit with slower kinetics of assembly than that witnessed for wild-type E-cadherin.¹⁵ The ambiguity in the role of the basic residue at position 14 in the kinetics of dimerization in classical cadherins provides ample opportunity for future studies on the nature of the intermediate structure.

When this article was in final revision, a crystal structure of the W2F mutant of NCAD12 was published (PDB ID: 4NUQ⁴⁵). The side chain of R14 in this structure is unstructured, supporting the idea that it is not involved in stabilization of the purported X-interface.

■ ASSOCIATED CONTENT

● Supporting Information

Thermal denaturation data and results of analysis of the first transition and analytical SEC data for X-enabled and X-enabled/R14E mutants. This material is available free of charge via the Internet at <http://pubs.acs.org>.

■ AUTHOR INFORMATION

Corresponding Author

*Phone: 1-662-915-7561; Fax: 1-662-915-7300; E-mail: nvunnam@olemiss.edu.

Funding

This work was supported by grant MCB 0950494 from the National Science Foundation.

Notes

The authors declare no competing financial interest.

■ ACKNOWLEDGMENTS

The authors gratefully acknowledge the peer review process and the insightful comments of the reviewers.

■ ABBREVIATIONS

Apo, calcium-depleted; EC1, extracellular domain 1; EC2, extracellular domain 2; ECAD12, epithelial-cadherin domains 1 and 2 (residues 1–219); EDTA, ethylenediaminetetraacetic acid; HEPES, *N*-(2-hydroxyethyl) piperazine-*N'*-2-ethanesulfonic acid; NCAD12, neural-cadherin domains 1 and 2 (residues 1–221); NCAD12/X-enabled, NCAD12/M101Q/P138D/N198E; NCAD12/X-enabled/R14E, NCAD12 with X-enabled mutant and arginine to glutamate mutant; SDS-PAGE, sodium dodecyl sulfate polyacrylamide gel electrophoresis; SEC, size-exclusion chromatography

■ REFERENCES

- (1) Bekirov, I. H., Needleman, L. A., Zhang, W., and Benson, D. L. (2002) Identification and localization of multiple classic cadherins in developing rat limbic system. *Neuroscience* 115, 213–227.
- (2) Redies, C. (2000) Cadherins in the central nervous system. *Prog. Neurobiol.* 61, 611–648.

- (3) Hirano, S., Suzuki, S. T., and Redies, C. (2003) The cadherin superfamily in neural development: diversity, function and interaction with other molecules. *Front. Biosci.* 8, d306–355.

- (4) Bozdagi, O., Shan, W., Tanaka, H., Benson, D. L., and Huntley, G. W. (2000) Increasing numbers of synaptic puncta during late-phase LTP: N-cadherin is synthesized, recruited to synaptic sites, and required for potentiation. *Neuron* 28, 245–259.

- (5) Fannon, A. M., and Colman, D. R. (1996) A model for central synaptic junctional complex formation based on the differential adhesive specificities of the cadherins. *Neuron* 17, 423–434.

- (6) Manabe, T., Togashi, H., Uchida, N., Suzuki, S. C., Hayakawa, Y., Yamamoto, M., Yoda, H., Miyakawa, T., Takeichi, M., and Chisaka, O. (2000) Loss of cadherin-11 adhesion receptor enhances plastic changes in hippocampal synapses and modifies behavioral responses. *Mol. Cell. Neurosci.* 15, 534–546.

- (7) Mariotti, A., Perotti, A., Sessa, C., and Ruegg, C. (2007) N-cadherin as a therapeutic target in cancer. *Expert Opin. Invest. Drugs* 16, 451–465.

- (8) Katsamba, P., Carroll, K., Ahlsen, G., Bahna, F., Vendome, J., Posy, S., Rajebhosale, M., Price, S., Jessell, T. M., Ben-Shaul, A., Shapiro, L., and Honig, B. H. (2009) Linking molecular affinity and cellular specificity in cadherin-mediated adhesion. *Proc. Natl. Acad. Sci. U.S.A.* 106, 11594–11599.

- (9) Vunnam, N., Flint, J., Balbo, A., Schuck, P., and Pedigo, S. (2011) Dimeric states of neural- and epithelial-cadherins are distinguished by the rate of disassembly. *Biochemistry* 50, 2951–2961.

- (10) Yagi, T., and Takeichi, M. (2000) Cadherin superfamily genes: functions, genomic organization, and neurologic diversity. *Genes Dev.* 14, 1169–1180.

- (11) Angst, B. D., Marcozzi, C., and Magee, A. I. (2001) The cadherin superfamily: diversity in form and function. *J. Cell Sci.* 114, 629–641.

- (12) Nollet, F., Kools, P., and van Roy, F. (2000) Phylogenetic analysis of the cadherin superfamily allows identification of six major subfamilies besides several solitary members. *J. Mol. Biol.* 299, 551–572.

- (13) Posy, S., Shapiro, L., and Honig, B. (2008) Sequence and structural determinants of strand swapping in cadherin domains: do all cadherins bind through the same adhesive interface? *J. Mol. Biol.* 378, 954–968.

- (14) Koch, A. W., Manzur, K. L., and Shan, W. (2004) Structure-based models of cadherin-mediated cell adhesion: the evolution continues. *Cell. Mol. Life Sci.* 61, 1884–1895.

- (15) Harrison, O. J., Bahna, F., Katsamba, P. S., Jin, X., Brasch, J., Vendome, J., Ahlsen, G., Carroll, K. J., Price, S. R., Honig, B., and Shapiro, L. (2010) Two-step adhesive binding by classical cadherins. *Nat. Struct. Mol. Biol.* 17, 348–357.

- (16) Hong, S., Troyanovsky, R. B., and Troyanovsky, S. M. (2011) Cadherin exits the junction by switching its adhesive bond. *J. Cell Biol.* 192, 1073–1083.

- (17) Li, Y., Altorelli, N. L., Bahna, F., Honig, B., Shapiro, L., and Palmer, A. G., III. (2013) Mechanism of E-cadherin dimerization probed by NMR relaxation dispersion. *Proc. Natl. Acad. Sci. U.S.A.* 110, 16462–16467.

- (18) Baumgartner, W., Golenhofen, N., Grundhofer, N., Wiegand, J., and Drenckhahn, D. (2003) Ca²⁺ dependency of N-cadherin function probed by laser tweezer and atomic force microscopy. *J. Neurosci.* 23, 11008–11014.

- (19) Perret, E., Benoliel, A. M., Nassoy, P., Pierres, A., Delmas, V., Thiery, J. P., Bongrand, P., and Feracci, H. (2002) Fast dissociation kinetics between individual E-cadherin fragments revealed by flow chamber analysis. *EMBO J.* 21, 2537–2546.

- (20) Perret, E., Leung, A., Feracci, H., and Evans, E. (2004) Trans-bonded pairs of E-cadherin exhibit a remarkable hierarchy of mechanical strengths. *Proc. Natl. Acad. Sci. U.S.A.* 101, 16472–16477.

- (21) Mysore, S. P., Tai, C. Y., and Schuman, E. M. (2008) N-cadherin, spine dynamics, and synaptic function. *Front. Neurosci.* 2, 168–175.

- (22) Vunnam, N., and Pedigo, S. (2012) X-interface is not the explanation for the slow disassembly of N-cadherin dimers in the apo state. *Protein Sci.* 21, 1006–1014.
- (23) Sivasankar, S., Zhang, Y., Nelson, W. J., and Chu, S. (2009) Characterizing the initial encounter complex in cadherin adhesion. *Structure* 17, 1075–1081.
- (24) Tamura, K., Shan, W. S., Hendrickson, W. A., Colman, D. R., and Shapiro, L. (1998) Structure–function analysis of cell adhesion by neural (N-) cadherin. *Neuron* 20, 1153–1163.
- (25) Vunnam, N., and Pedigo, S. (2011) Calcium-induced strain in the monomer promotes dimerization in neural cadherin. *Biochemistry* 50, 8437–8444.
- (26) Chen, C. P., Posy, S., Ben-Shaul, A., Shapiro, L., and Honig, B. H. (2005) Specificity of cell–cell adhesion by classical cadherins: critical role for low-affinity dimerization through beta-strand swapping. *Proc. Natl. Acad. Sci. U.S.A.* 102, 8531–8536.
- (27) Ciatto, C., Bahna, F., Zampieri, N., VanSteenhouse, H. C., Katsamba, P. S., Ahlsen, G., Harrison, O. J., Brasch, J., Jin, X., Posy, S., Vendome, J., Ranscht, B., Jessell, T. M., Honig, B., and Shapiro, L. (2010) T-cadherin structures reveal a novel adhesive binding mechanism. *Nat. Struct. Mol. Biol.* 17, 339–347.
- (28) Pace, C. N., Vajdos, F., Fee, L., Grimsley, G., and Gray, T. (1995) How to measure and predict the molar extinction coefficient of a protein. *Protein Sci.* 4, 2411–2423.
- (29) Prasad, A., Housley, N. A., and Pedigo, S. (2004) Thermodynamic stability of domain 2 of epithelial cadherin. *Biochemistry* 43, 8055–8066.
- (30) Vunnam, N., McCool, J. K., Williamson, M., and Pedigo, S. (2011) Stability studies of extracellular domain two of neural-cadherin. *Biochim. Biophys. Acta* 14, 1841–1845.
- (31) Vunnam, N., and Pedigo, S. (2011) Prolines in betaA-sheet of neural cadherin act as a switch to control the dynamics of the equilibrium between monomer and dimer. *Biochemistry* 50, 6959–6965.
- (32) Nagar, B., Overduin, M., Ikura, M., and Rini, J. M. (1996) Structural basis of calcium-induced E-cadherin rigidification and dimerization. *Nature* 380, 360–364.
- (33) Emond, M. R., Biswas, S., Blevins, C. J., and Jontes, J. D. (2011) A complex of protocadherin-19 and N-cadherin mediates a novel mechanism of cell adhesion. *J. Cell Biol.* 195, 1115–1121.
- (34) Kudo, S., Caaveiro, J. M., Goda, S., Nagatoishi, S., Ishii, K., Matsuura, T., Sudou, Y., Kodama, T., Hamakubo, T., and Tsumoto, K. (2014) Identification and characterization of the X-dimer of human P-cadherin: implications for homophilic cell adhesion. *Biochemistry* 53, 1742–1752.
- (35) Brown, E. M., Vassilev, P. M., and Hebert, S. C. (1995) Calcium ions as extracellular messengers. *Cell* 83, 679–682.
- (36) Rusakov, D. A., and Fine, A. (2003) Extracellular Ca²⁺ depletion contributes to fast activity-dependent modulation of synaptic transmission in the brain. *Neuron* 37, 287–297.
- (37) Gerweck, L. E., and Seetharaman, K. (1996) Cellular pH gradient in tumor versus normal tissue: potential exploitation for the treatment of cancer. *Cancer Res.* 56, 1194–1198.
- (38) Stuwe, L., Muller, M., Fabian, A., Waning, J., Mally, S., Noel, J., Schwab, A., and Stock, C. (2007) pH dependence of melanoma cell migration: protons extruded by NHE1 dominate protons of the bulk solution. *J. Physiol.* 585, 351–360.
- (39) Perilli, G., Saracini, C., Daniels, M. N., and Ahmad, A. (2013) Diabetic ketoacidosis: a review and update. *Curr. Emerg. Hosp. Med. Rep.* 1, 10–17.
- (40) Adeva-Andany, M., López-Ojén, M., Funcasta-Calderón, R., Ameneiros-Rodríguez, A., Donapetry-García, C., Vila-Altesor, M., and Rodríguez-Seijas, J. (2014) Comprehensive review on lactate metabolism in human health. *Mitochondrion* 17, 76–100.
- (41) Fencil, V., Jabor, A., Kazda, A., and Figge, J. (2000) Diagnosis of metabolic acid-base disturbances in critically ill patients. *Am. J. Respir. Crit. Care Med.* 162, 2246–2251.
- (42) Ziemann, A. E., Allen, J. E., Dahdaleh, N. S., Drebot, I. L., Coryell, M. W., Wunsch, A. M., Lynch, C. M., Faraci, F. M., Howard, M. A., III, Welsh, M. J., and Wemmie, J. A. (2009) The amygdala is a chemosensor that detects carbon dioxide and acidosis to elicit fear behavior. *Cell* 139, 1012–1021.
- (43) Magnotta, V. A., Heo, H. Y., Dlouhy, B. J., Dahdaleh, N. S., Follmer, R. L., Thedens, D. R., Welsh, M. J., and Wemmie, J. A. (2012) Detecting activity-evoked pH changes in human brain. *Proc. Natl. Acad. Sci. U.S.A.* 109, 8270–8273.
- (44) Prozialeck, W. C., Grunwald, G. B., Dey, P. M., Reuhl, K. R., and Parrish, A. R. (2002) Cadherins and NCAM as potential targets in metal toxicity. *Toxicol. Appl. Pharmacol.* 182, 255–265.
- (45) Vendome, J., Felsovalyi, K., Song, H., Yang, Z., Jin, X., Brasch, J., Harrison, O. J., Ahlsen, G., Bahna, F., Kaczynska, A., Katsamba, P. S., Edmond, D., Hubbell, W. L., Shapiro, L., and Honig, B. (2014) Structural and energetic determinants of adhesive binding specificity in type I cadherins. *Proc. Natl. Acad. Sci. U.S.A.* 111, E4175–4184.
- (46) Pertz, O., Bozic, D., Koch, A. W., Fauser, C., Brancaccio, A., and Engel, J. (1999) A new crystal structure, Ca²⁺ dependence and mutational analysis reveal molecular details of E-cadherin homoassociation. *EMBO J.* 18, 1738–1747.